Induction of Thermotropic Liquid Crystalline Phases in Coil−Rod−Coil Triblock Molecules Containing Poly(propylene oxide) through Complexation with $LiCF_3SO_3$

Myongsoo Lee* and Byoung-Ki Cho

Department of Chemistry, Yonsei University, Shinchon 134, Seoul 120-749, Korea

Received February 5, 1998. Revised Manuscript Received April 27, 1998

The preparation and thermotropic phase behavior of coil−rod−coil triblock molecules of dodecyl 4-(4-oxy-4′-biphe nylcarbonyloxy)-4′-biphenylcarboxylate with poly(propylene oxide) of seven (**7-22)** and twelve (**12-22)** propylene oxide subunits and the complexes of the triblock molecules with $LiCF_3SO_3$ are presented. Both **7-22** and **12-22** appear to be only crystalline solid. However, the complexation of **7-22** and **12-22** with $LiCF_3SO_3$ induces an enantiotropic liquid crystalline phase. The complexes of **7-22** with 0.05−0.20 mol of $LiCF_3SO_3$ per propylene oxide unit of a molecule exhibit an enantiotropic smectic A mesophase. In contrast, a significant phase change is observed upon complexation of **12-22** with $LiCF_3SO_3$. The complex of **12-22** with 0.10 mol of $LiCF_3SO_3$ exhibits a smectic A mesophase. However, the complexes with 0.15−0.30 mol of $LiCF_3SO_3$ display a hexagonal columnar mesophase. The thermal stability of the mesophase exhibited by the lithium complexes based on each triblock molecule increases with increasing salt concentration. This behavior is attributed to the dynamics of ionic association resulting from specific interactions between the ether oxygens and the cations. These results, characterized by a combination of techniques consisting of differential scanning calorimetry, thermal optical microscopy, and Raman spectroscopy, are discussed.

Introduction

One of the most fascinating properties of rod−coil molecules consisting of a rigid rod and a flexible coil is their ability to microphase separate into a rich variety of ordered microstructures. Theoretical investigations have been made of the phase behavior of rod−coil diblock molecules. These investigations have predicted nematic−smectic A and smectic A−smectic C transitions in the melt state.[1] Other theoretical work has also predicted not only the familiar lamellar phase but also various micellar phases for a sufficiently large coil volume fraction.[2]

Experimentally, rod−coil molecules based on poly(hexyl isocyanate) have been reported to exhibit zigzag lamellar structures,[3] while other rod−coil molecules based on an extended molecular rod have been found to display lamellar or micellar structures, depending on the coil volume fraction of the molecules.[4] Recently our publications[5] have shown that rod−coil molecules consisting of a molecular rod and a poly(ethylene oxide) coil exhibit a microphase-separated lamellar structure with nanoscale dimensions in the crystalline phase as well as in the melt state. In a more recent experiment, we have also introduced a bulkier poly(propylene oxide) as a flexible coil into a molecular rod. In this case, the rod−coil molecules appear to display successively lamellar smectic A, cubic, and cylindrical micellar mesophases as a function of coil volume fraction.[6]

Poly(alkylene oxide) has several advantages, particularly due to its complexation capability with alkali metal cations, which can provide an application potential for solid polyelectrolytes[7] and induce various liquid crystalline supramolecular structures.[8] Recent work on poly(ethylene oxide) with flexible side groups has shown that complexation of polymer backbones with $LiClO_4$ induces

* To whom all correspondence should be addressed.

(1) (a) Semenov, A. N.; Vasilenko, S. V. *Sov. Phys. JEPT (Engl. Transl.)* **1986**, *63*, 70. (b) Semenov, A. N. *Mol. Cryst. Liq. Cryst.* **1991**, *209*, 191.

(2) (a) Halperin, A. *Macromolecules* **1990**, *23*, 2724. (b) Williams, D. R. M.; Fredrickson G. H. *Macromolecules* **1992**, *25*, 3561.

(3) (a) Chen, J. T.; Thomas, E. L.; Ober, C. K.; Hwang, S. S. *Macromolecules* **1995**, *28*, 1688. (b) Chen, J. T.; Thomas, E. L.; Ober, C. K.; Mao, G.-P. *Science* **1996**, *273*, 343.

(4) (a) Radzilowski, L. H.; Stupp, S. I. *Macromolecules* **1994**, *27*, 7747. (b) Radzilowski, L. H.; Carragher, B. O.; Stupp, S. I. *Macromolecules* **1997**, *30*, 2110. (c) Stupp, S. I.; LeBonheur, V.; Walker, K.; Li, L. S.; Huggins, K. E.; Keser, M.; Amstutz, A. *Science* **1997**, *276*, 384.

(5) (a) Lee, M.; Oh, N.-K. *J. Mater. Chem.* **1996**, *6*, 1079. (b) Lee, M.; Oh, N.-K.; Lee, H.-K.; Zin, W.-C. *Macromolecules* **1996**, *29*, 5567.

(6) (a) Lee, M.; Oh, N.-K.; Zin, W.-C. *Chem. Commun.* **1996**, 1787. (b) Lee, M.; Cho, B.-K.; Kim, H.; Zin, W.-C. *Angew. Chem., Int. Ed. Engl.* **1998**, *37*, 638.

(7) (a) Thatcher, J. H.; Thanapprapasr, K.; Nagae, S.; Mai, S.-M.; Booth, C.; Owen, J. R. *J. Mater. Chem.* **1994**, *4*, 591. (b) Takabe, Y.; Hochi, K.; Matsuba, T.; Shirota, Y. *J. Mater. Chem.* **1994**, *4*, 599. (c) LeNest, J. F.; Ghandini, A.; Schoenenberger, C. *Trends Polym. Sci.*, **1994**, *2*, 32.

(8) (a) Dias, F. B.; Voss, T. P.; Batty, S. V.; Wright, P. V.; Ungar, G. *Macromol. Rapid Commun.* **1994**, *15*, 961. (b) Percec, V.; Heck, J.; Johansson, G.; Tomazos, D.; Ungar, G. *Macromol. Symp.* **1994**, *77*, 237 and references therein.

S0897-4756(98)00070-2 CCC: $15.00
Published on Web 06/13/1998

a smectic lamellar mesophase from a crystalline phase of uncomplexed polymer.[8a] Experimental work on taper-shaped molecules containing oligo(ethylene oxide) has also demonstrated that complexation of the molecules with alkali metal trifluoromethanesulfonate could induce a hexagonal columnar mesophase.[8b]

Recently, we have shown that the control of the supramolecular structure in rod−coil molecular systems containing poly(ethylene oxide) from lamellar, cubic to cylindrical phases is possible through complexation with lithium ion.[5b,9] Induction of the supramolecular structures with curved interfaces from rodlike molecules has been suggested to be due to an increase of the coil volume fraction resulting from the selective solvation of added salts in the microphase-segragated poly(ethylene oxide) segments, which requires new supramolecular structures for reducing space crowding of coil segments.[9]

As an extension of this work, we have investigated the effect of the lithium complexation on the phase behavior of coil−rod−coil triblock molecules based on poly(propylene oxide). We have synthesized coil−rod−coil ABC triblock molecules where the rod is 4-[4-oxy-4′-biphenylcarbonyloxy]-4′-biphenylcarboxylate and the coils are docosyl group as the A block and poly(propylene oxide) with average lengths of 7 (**7-22**) and 12 (**12-22**) propylene oxide subunits as the C block, respectively. The complexes of coil−rod−coil triblock molecules with $LiCF_3SO_3$ have also been prepared to investigate their phase change upon complexation. The goal of this paper

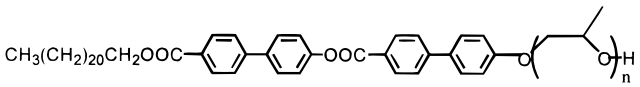

n=7 (**7-22**)
n=12 (**12-22**)

is to describe the synthesis of these coil−rod−coil triblock molecules and their phase change upon complexation with $LiCF_3SO_3$. The mesomorphic phase behavior as characterized by a combination of techniques consisting of differential scanning calorimetry (DSC) and thermal optical polarized microscopy is described, and the role of the added lithium trifluoromethanesulfonate (triflate) in the coil−rod−coil system as characterized by Raman spectroscopy is also discussed.

Experimental Section

Materials. 4-Hydroxy-4′-biphenylcarboxylic acid (98%), 1-bromodocosane (96%), 1, 3-diisopropylcarbodiimide (DIPC, 99%), toluene-*p*-sulfonyl chloride (98%), 4-(dimethylamino)-pyridine (99%), poly(propylene glycol) of M_w 425 and 725 (all from Aldrich), and the other conventional reagents were used as received. 4-Dimethylaminopyridinium-*p*-toluene sulfonate (DPTS) was prepared as described previously[10] and dried under vacuum at 50 °C for 48 h. Ethyl 4-hydroxy-4′-biphenylcarboxylate was also prepared as described previously.[5a] Dichloromethane was dried by distillation from calcium hydride and stored over 4-Å molecular sieves. Pyridine was dried by distillation from sodium metal and stored over 4-Å molecular sieves.

Techniques. ^{1}H NMR spectra were recorded from $CDCl_3$ solutions on a Bruker AM 250 spectrometer. The purity of the products was checked by thin-layer chromatography (TLC; Merck, silica gel 60). A Perkin-Elmer DSC-7 differential scanning calorimeter equipped with a 1020 thermal analysis controller was used to determine the thermal transitions, which were reported as the maxima and minima of their endothermic or exothermic peaks. In all cases, the heating and cooling rates were 10 °C min^{-1}. A Nikon Optiphot 2-pol optical polarized microscopy (magnification: 100×) equipped with a Mettler FP 82 hot-stage and a Mettler FP 90 central processor was used to observe the thermal transitions and to analyze the anisotropic texture.[11] Microanalyses were performed with a Perkin-Elmer 240 elemental anlayzer at Korea Research Institute of Chemical Technology. Raman spectra were obtained using Reinshaw Raman microsystem 2000. A He−Ne laser with a wavelength of 632.8 nm was used as excitation. The laser output power was maintained at 5 mW, and spectral resolution was maintained at 2 cm^{-1}. X-ray scattering measurements were performed in transmission mode with synchrotron radiation at the 4C2 X-ray beam line at Pohang Accelerator Laboratory, Korea. To investigate structural changes on heating, the sample was held in an aluminum sample holder which was sealed with a window of 7 mm thick Kapton films on both sides. The sample was heated with two catridge heaters, and the temperature of the samples was monitored by a thermocouple placed close to the sample. Background scattering correction was made by subtracting the scattering from the Kapton. Molecular weight distributions (M_w/M_n) were determined by gel permeation chromatography (GPC) with a Waters R401 instrument equipped with Stragel HR 3, 4, and 4E columns, an M7725i manual injector, a column heating chamber, and a 2010 Millennium data station. Measurements were made by using a UV detector and $CHCl_3$ as solvent (1.0 mL min^{-1}).

Synthesis. The synthesis of coil−rod−coil triblock molecules with different coil lengths is outlined in Scheme 1.

Synthesis of Compounds 3 and 4. Oxypoly(propyleneoxy)propyl tosylate **3** and **4** were synthesized using the same procedure. A representative example is described for **4**. Poly(propylene glycol) (M_w 725, 50.0 g, 68.9 mmol) was dissolved in 150 mL of dry methylene chloride under nitrogen. A solution of toluene-*p*-sulfonyl chloride (45.3 g, 237.6 mmol) in 70 mL of dry methylene chloride was added under nitrogen. Dry pyridine (6.27 mL, 77.6 mmol) was then added dropwise to the mixture. The reaction mixture was stirred at room temperature under nitrogen overnight. The methylene chloride solution was washed with water, dried over anhydrous magnesium sulfate, and filtered. The solvent was removed in a rotary evaporator, and the crude product was purified by column chromatography (silica gel, ethyl acetate eluent) to yield 16.4 g (27.0%) of a colorless liquid.

Compound 3. Yield 26.7%. ^{1}H NMR (250 MHz, $CDCl_3$) δ 7.80 (d, 2Ar−H, *o* to SO_3, J = 8.1 Hz), 7.31 (d, 2Ar−H, *o* to CH_3, J = 8.0 Hz), 4.65 (m, $CH_2CH(CH_3)$O-phenyl or $(CH_3)CHCH_2$O-phenyl), 3.14−3.91 (m, $OCH_2CH(CH_3)$), 2.43 (s, 3H, CH_3-phenyl), 0.99−1.28 (m, 21H, $OCH_2CH(CH_3)$).

Compound 4. Yield 27.0%. ^{1}H NMR (250 MHz, $CDCl_3$) δ 7.77 (d, 2Ar−H, *o* to SO_3, J = 8.2 Hz), 7.31 (d, 2Ar−H, *o* to CH_3, J = 7.9 Hz), 4.63 (m, $CH_2CH(CH_3)$O-phenyl or $(CH_3)CHCH_2$O-phenyl), 3.17−3.94 (m, $OCH_2CH(CH_3)$), 2.43 (s, 3H, CH_3-phenyl), 0.95−1.20 (m, 36H, $OCH_2CH(CH_3)$).

Synthesis of Compound 5 and **6.** 4-[Oxy poly(propyleneoxy)propyloxy]-4′-biphenylcarboxylic acids **5** and **6** were synthesized using the same procedure. A representative example is described for **6**. Compound **4** (10.0 g, 11.3 mmol), ethyl 4-hydroxy-4′-biphenylcarboxylate (8.2 g, 33.9 mmol), and

(9) (a) Lee, M.; Oh, N.-K. *Mol. Cryst. Liq. Cryst.* **1996**, *280*, 283. (b) Lee, M.; Zin, W.-C.; Ji, S. H. *Bull. Kor. Chem. Soc.* **1996**, *17*, 309. (c) Lee, M.; Oh, N.-K.; Choi, M.-G. *Polym. Bull.* **1996**, *37*, 511.

(10) Moor, J. S.; Stupp, S. I. *Macromolecules* **1990**, *23*, 65.

(11) (a) Demus, D.; Richter, L. *Texture of Liquid Crystals*; Verlag Chemie: Weinheim, Germany, 1978. (b) Gray, G. W.; Goodby, J. W. *Smectic Liquid Crystals. Textures and Structures*; Leonard Hill, Glasgow, Great Britain, 1984.

Scheme 1. Synthesis of Coil−rod−coil Molecules 7-22 and 12-22

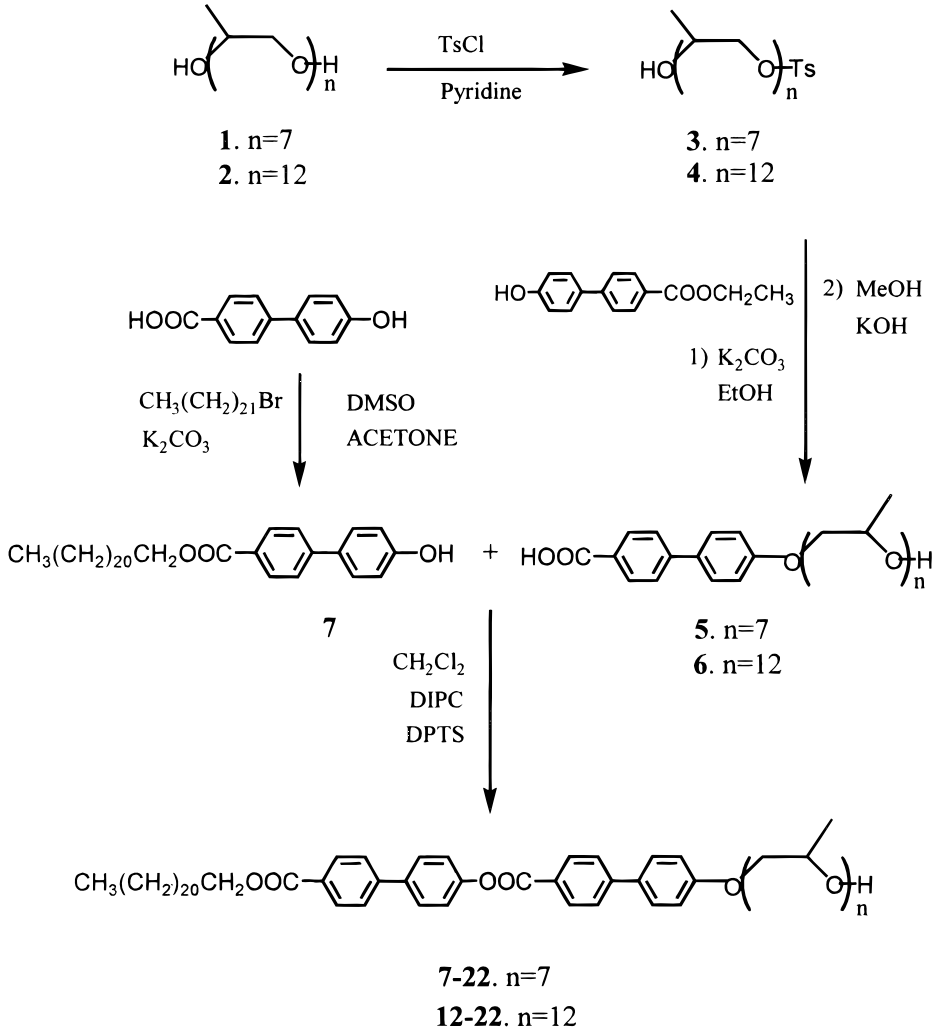

excess K_2CO_3 were dissolved in 250 mL of ethanol. The mixture was heated at reflux for 24 h and then cooled to room temperature, and excess KOH was added. The mixture was stirred at room temperature for 3 h. The resulting solution was poured into water and extracted with methylene chloride. The methylene chloride solution was washed with water, dried over anhydrous magnesium sulfate, and filtered. Solvent removal in a rotary evaporator yielded 6.7 g (64.0%) of a colorless liquid.

Compound 5. Yield 60.2%. ^{1}H NMR (250 MHz, $CDCl_3$) δ 8.13 (d, 2Ar−H, *o* to COOH, J = 8.4 Hz), 7.64 (d, 2Ar−H, *m* to COOH, J = 8.4 Hz), 7.55 (d, 2Ar−H, *m* to $OCH_2CH(CH_3)$, J = 8.7 Hz), 7.02 (d, 2Ar−H, *o* to $OCH_2CH(CH_3)$, J = 8.5 Hz), 4.57 (m, $CH_2CH(CH_3)$O-phenyl or $(CH_3)CHCH_2$O-phenyl), 3.15−4.00 (m, $OCH_2CH(CH_3)$, 0.85−1.37 (m, 21H, $OCH_2CH(CH_3)$). Anal. Calcd for $C_{34}H_{52}O_{10}$: C, 65.78; H, 8.44. Found: C, 65.88; H, 8.52.

Compound 6. Yield 64.0%. ^{1}H NMR (250 MHz, $CDCl_3$) δ 8.12 (d, 2Ar−H, *o* to COOH, J = 8.5 Hz), 7.58 (d, 2Ar−H, *m* to COOH, J = 8.5 Hz), 7.52 (d, 2Ar−H, *m* to $OCH_2CH(CH_3)$, J = 8.5 Hz), 6.99 (d, 2Ar−H, *o* to $OCH_2CH(CH_3)$, J = 8.5 Hz), 4.56 (m, $CH_2CH(CH_3)$O-phenyl or $(CH_3)CHCH_2$O-phenyl), 3.15−4.05 (m, $OCH_2CH(CH_3)$, 0.85−1.37 (m, 36H, $OCH_2CH(CH_3)$). Anal. Calcd for $C_{49}H_{82}O_{15}$: C, 64.59; H, 9.07. Found: C, 64.48; H, 9.17.

Synthesis of Compound 7. 4-Hydroxy-4′-biphenylcarboxylic acid (3.0 g, 14.0 mmol), 1-bromodocosane (16.0 g, 42.0 mmol), and K_2CO_3 (1.1 g, 7.0 mmol) were dissolved in 150 mL of acetone and 20 mL of dimethyl sulfoxide (DMSO). The mixture was heated at reflux for 36 h and then cooled to room temperature and acidified with 1 N HCl. The resulting solution was poured into water and extracted with methylene chloride. The methylene chloride solution was washed with water, dried over anhydrous magnesium sulfate, and filtered. The solvent was removed in a rotary evaporator, and the crude product was then purified by recrystallization sequentially from methanol and hexane to yield 2.1 g (29.0%) of a white solid. ^{1}H NMR (250 MHz, $CDCl_3$) δ 8.06 (d, 2Ar−H, *o* to COO, J = 8.3 Hz), 7.62 (d, 2Ar−H, *m* to COO, J = 8.3 Hz), 7.53 (d, 2Ar−H, *m* to OH, J = 8.3 Hz), 6.95 (d, 2Ar−H, *o* to OH, J = 8.3 Hz), 4.35 (t, 2H, $CH_3(CH_2)_{20}CH_2$, J = 6.6 Hz), 1.77 (m, 2H, $CH_3(CH_2)_{19}CH_2$), 1.24−1.47 (m, 38H, $CH_3(CH_2)_{19}$), 0.87 (t, 3H, $CH_3(CH_2)_{19}CH_2$, J = 6.8 Hz). Anal. Calcd for $C_{35}H_{54}O_3$: C, 80.41; H, 10.41. Found: C, 80.39; H, 10.35.

Synthesis of Coil−Rod−Coil Molecules 7-22 and 12-22. Docosyl 4-[4-[oxy poly(propyleneoxy)propyloxy]-4′-biphenylcarboxyloxy]-4′-biphenylcarboxylates **7-22** and **12-22** were synthesized using the same procedure. A representative example is described for **12-22**. Compound **6** (0.40 g, 0.43 mmol), docosyl 4-hydroxy-4′-biphenylcarboxylate (0.45 g, 0.86 mmol), and 4-dimethylaminopyridinium-*p*-toluene sulfonate (DPTS, 0.63 g, 2.1 mmol) were dissolved in 100 mL of dry methylene chloride under nitrogen. 1,3-Diisopropylcarbodiimide (DIPC, 0.14 mL, 0.86 mL) was then added dropwise to the mixture. The mixture was stirred at room temperature under nitrogen overnight. The resulting solution was poured into water and extracted with methylene chloride. The methylene chloride solution was washed with water, dried over anhydrous magnesium sulfate, and filtered. The solvent was removed in a rotary evaporator, and the crude product was purified by column chromatography (silica gel, ethyl acetate) to yield 0.3 g (49.0%) of a white solid.

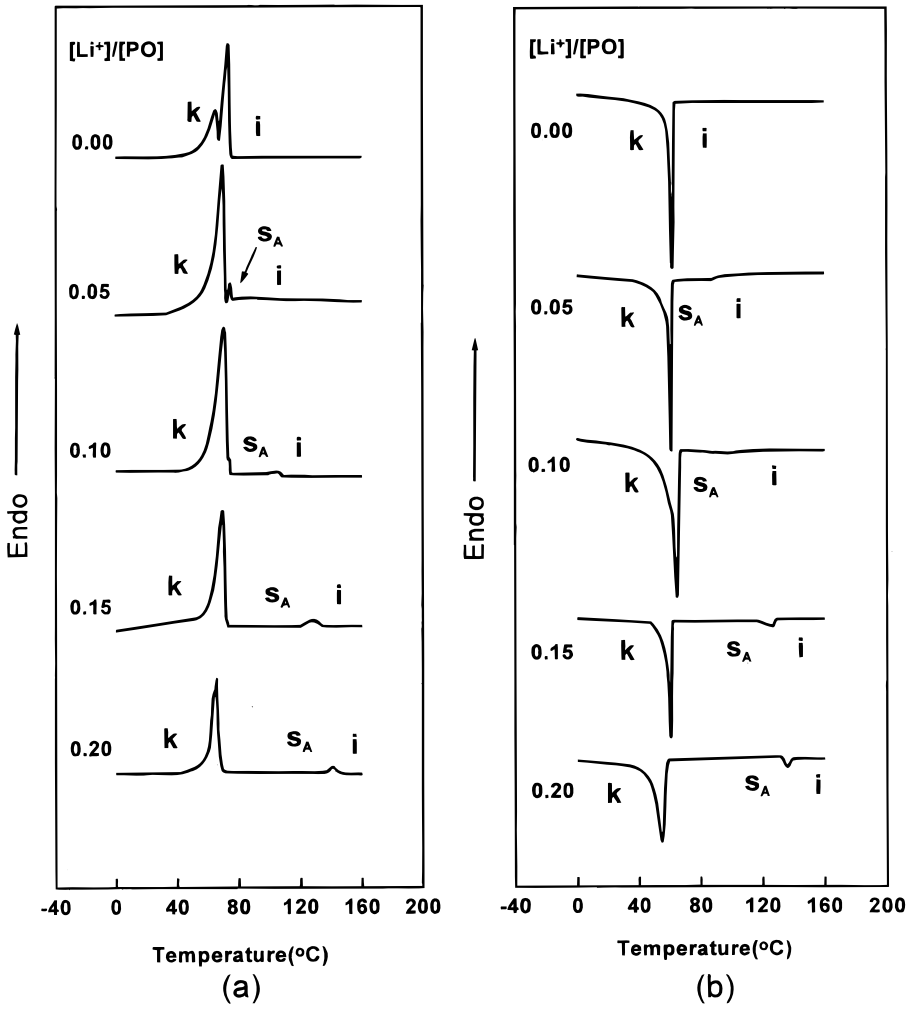

Figure 1. DSC traces (10 °C min^{-1}) recorded during the heating scan (a) and the cooling scan (b) of **7-22**.

7-22. Yield 45.8%. ^{1}H NMR (250 MHz, $CDCl_3$) δ 8.26 (d, 2Ar−H, *o* to COO-phenyl, J = 8.2 Hz), 8.13 (d, 2Ar−H, *o* to $COOCH_2$, J = 8.2 Hz), 7.65−7.72 (m, 6Ar−H, *m* to COO-phenyl, *m* to biphenylcarboxylate, and *m* to $COOCH_2$), 7.59 (d, 2Ar−H, *m* to $OCH_2CH(CH_3)$, J = 8.6 Hz), 7.34 (d, 2Ar−H, *o* to biphenylcarboxylate, J = 8.4 Hz), 7.04 (d, 2Ar−H, *o* to $OCH_2CH(CH_3)$, J = 8.3 Hz), 4.58 (m, $CH_2CH(CH_3)$O-phenyl or $(CH_3)CHCH_2$O-phenyl), 4.34 (t, 2H, $CH_3(CH_2)_{20}CH_2$, J = 6.6 Hz), 3.18−3.92 (m, $OCH_2CH(CH_3)$), 1.77 (m, 2H, $CH_3(CH_2)_{19}CH_2$), 1.25−1.40 (m, 41H, $CH_3(CH_2)_{19}$ and $CH(CH_3)$O-phenyl), 1.08−1.18 (m, 18H, $OCH_2CH(CH_3)$), 0.88 (t, 3H, $CH_3(CH_2)_{21}$, J = 6.8 Hz). M_w/M_n = 1.10 (GPC). Anal. Calcd for $C_{69}H_{104}O_{12}$: C, 73.63; H, 9.31. Found: C, 73.81; H, 8.95.

12-22. Yield 49.0%. ^{1}H NMR (250 MHz, $CDCl_3$) δ 8.26 (d, 2Ar−H, *o* to COO-phenyl, J = 8.2 Hz), 8.13 (d, 2Ar−H, *o* to $COOCH_2$, J = 8.2 Hz), 7.65−7.72 (m, 6Ar−H, *m* to COO-phenyl, *m* to biphenylcarboxylate, and *m* to $COOCH_2$), 7.59 (d, 2Ar−H, *m* to $OCH_2CH(CH_3)$, J = 8.6 Hz), 7.34 (d, 2Ar−H, *o* to biphenylcarboxylate, J = 8.4 Hz), 7.04 (d, 2Ar−H, *o* to $OCH_2CH(CH_3)$, J = 8.3 Hz), 4.58 (m, $CH_2CH(CH_3)$O-phenyl or $(CH_3)CHCH_2$O-phenyl), 4.34 (t, 2H, $CH_3(CH_2)_{20}CH_2$, J = 6.6 Hz), 3.18−3.93 (m, $OCH_2CH(CH_3)$), 1.77 (m, 2H, $CH_3(CH_2)_{19}CH_2$), 1.28−1.40 (m, 41H, $CH_3(CH_2)_{19}$ and $CH(CH_3)$O-phenyl), 0.98−1.17 (m, 33H, $OCH_2CH(CH_3)$), 0.88 (t, 3H, $CH_3(CH_2)_{21}$, J = 6.8 Hz). M_w/M_n = 1.16 (GPC). Anal. Calcd for $C_{84}H_{134}O_{17}$: C, 71.25; H, 9.54. Found: C, 71.06; H, 9.62.

Preparation of the Complexes of *n*-22 with $LiCF_3SO_3$. Complexes of ***n*-22** with lithium triflate were prepared by mixing solutions of ***n*-22** (10 mg mL^{-1}) in dry methylene chloride with an appropriate volume of 0.724 mmol mL^{-1} salt in dry acetonitrile solution, followed by slow evaporation of the solvent under reduced pressure at room temperature and subsequent drying in a vacuum oven at 60 °C to maintain constant mass. The absence of the free salt was verified by optical polarized microscopy.

Results and Discussion

Synthesis of Coil−Rod−Coil Triblock Molecules. Scheme 1 outlines the synthesis of coil−rod−coil triblock molecules **7-22** and **12-22**. All intermediary compounds were synthesized by following procedures available in the literature.[5a] Commercially available poly(propylene oxides) (average degrees of polymerization (DP), 7 and 12) were used as starting materials for **7-22** and **12-22**, respectively. The appropriate poly(propylene oxide) reacted with toluene-*p*-sulfonyl chloride to give monotosylated derivatives. Substitution reaction of monotosylated poly(propylene oxide) with ethyl 4-hydroxy-4′-biphenylcarboxylate and then hydrolysis of the resulting product produced compounds **5** and **6**. The coil−rod−coil molecules **7-22** and **12-22** were obtained from the reaction of **5** and **6** with docosyl 4-hydroxy-4′-biphenylcarboxylate in CH_2Cl_2 in the presence of diisopropylcarbodiimide and 4-dimethylamino pyridinium-*p*-toluene sulfonate (DPTS). The obtained coil−rod−coil molecules were purified by column chromatography (silica gel) using ethyl acetate as eluent. Satisfactory analytical data were obtained for the coil−rod−coil

Table 1. Thermal Transitions of 7-22 and Its Complexes with Lithium Triflate

complex $[LiCF_3SO_3]$/[PO]	phase transitions (°C) and corresponding enthalpy changes (kJ/mol)[a]	
	heating	cooling
0.00	k 73.6 (46.5) i	i 61.9 (48.2) k
0.05	k 69.9 (27.7) s_A 87.4 (0.6) i	i 85.9 (0.6 s_A 60.9 (29.1) k
0.10	k 70.7 (22.4) s_A 103.5 (0.7) i	i 97.5 (0.7) s_A 64.8 (23.6) k
0.15	k 69.7 (14.4) s_A 127.8 (1.2) i	i 126.7 (1.2) s_A 60.6 (13.8) k
0.20	k 65.7 (10.4) s_A 140.8 (0.9) i	i 135.7 (0.9) s_A 54.7 (10.6) k

[a] k, crystalline; s_A, smectic A; i, isotropic.

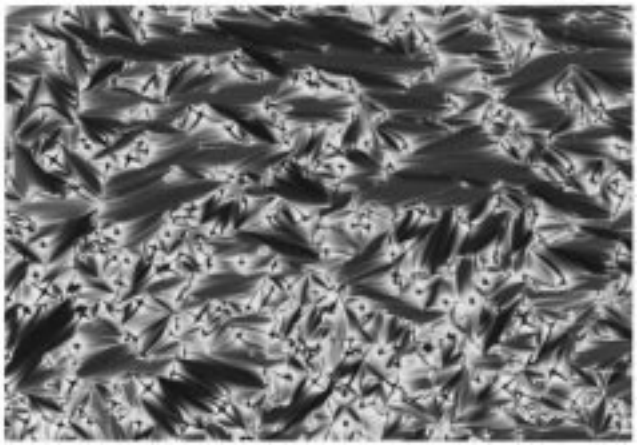

Figure 2. Representative optical polarized micrograph (65×) of the texture exhibited by the s_A mesophase of the complex of **7-22** with 0.05 mol of $LiCF_3SO_3$ at 85 °C on the cooling scan.

triblock molecules as given in the Experimental Section. We have investigated the phase change of **7-22** and **12-22** upon complexation with lithium triflate by a combination of techniques consisting of DSC and thermal optical polarized microscopy.

Thermal Behavior of the Complexes of 7-22 with $LiCF_3SO_3$. Figure 1 shows the DSC traces obtained from the heating (Figure 1a) and cooling scans (Figure 1b) of the coil−rod−coil molecule **7-22** and its complexes with 0.05−0.20 mol of $LiCF_3SO_3$ per propylene oxide unit of **7-22**. Table 1 summarizes the phase transitions and associated enthalpy changes of the complexes of **7-22** as a function of the amount of $LiCF_3SO_3$.

As shown in Table 1 and Figure 1, the coil−rod−coil molecule **7-22** is only crystalline, melting into an isotropic liquid at 73.6 °C. In contrast, the addition of lithium triflate results in formation of an enantiotropic mesophase. The complex with 0.05 mol of $LiCF_3SO_3$ per propylene oxide unit of **7-22** exhibits a crystalline melting transition followed by a smectic A mesophase on heating. On cooling from the isotropic liquid, first batonnet-like growth of texture can be observed, with a final development of focal conic domains which are characteristic of a smectic A mesophase displayed by conventional calamitic mesogens.[11] A representative texture of the smectic A phase exhibited by the complex with 0.05 mol of $LiCF_3SO_3$ is presented in Figure 2. The complex of **7-22** with 0.10 mol of $LiCF_3SO_3$ melts into a smectic A mesophase at 70.7 °C, and further heating gives rise to an isotropic liquid at 103.5 °C that presents a higher isotropization temperature than the complex with 0.05 mol of $LiCF_3SO_3$. The complexes with 0.15 and 0.20 mol of $LiCF_3SO_3$ resemble the phase behavior

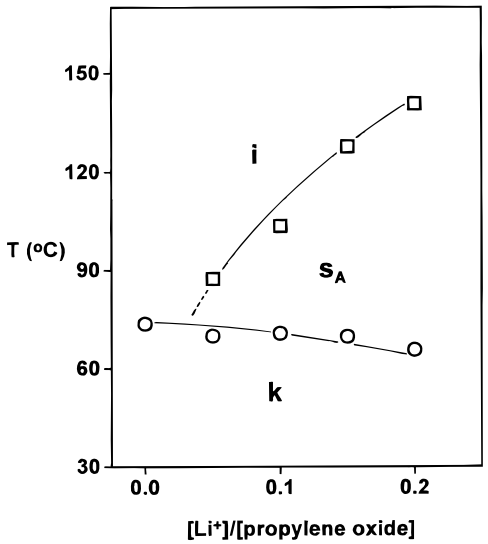

Figure 3. Dependence of phase-transition temperatures of **7-22** and its complexes with lithium triflate on $[LiCF_3SO_3]$/[propylene oxide]. Data are from the heating scan. (○) T_m; (□): T_i.

of the complex with 0.10 mol of $LiCF_3SO_3$ which exhibits an enantiotropic smectic A phase, except that their isotropic transitions are shifted toward higher temperatures (Table 1). Above a concentration of 0.20 mol of $LiCF_3SO_3$, the complex appears to become biphasic. Thermal optical polarized microscopy shows that both isotropic and anisotropic phases seem to coexist.

Figure 3 shows the dependence of the melting and isotropic transition temperatures obtained from the DSC heating scan as a function of the $LiCF_3SO_3$:propylene oxide subunit molar ratio. This figure demonstrates that the isotropization temperatures increase drastically with the increase in the salt concentration, while the crystalline melting transition temperatures are relatively constant within experimental error and independent of the salt concentration. As a consequence, the temperature range of the smectic A mesophase become broader as the salt concentration increases. This plot demonstrates that the added lithium triflate is selectively dissolved in the microphase-segregated poly(propylene oxide) coil segments since the crystalline melting transitions of the coil−rod−coil molecule appear to be very little dependent on the salt concentration. As expected for a kinetically controlled first-order transition, crystallization occurs at substantial supercooling (Table 1). On the other hand, the isotropic−s_A transition shows only slight supercooling which represents a thermodynamic effect. This is an expected behavior for a liquid crystalline phase.[12]

Another unique feature observed in these complexes is the dramatic decrease in the enthalpy change of crystalline melting as the salt concentration increases, as shown in Table 1. This can be attributed to the presence of ester oxygens of the rod blocks. As salt concentration increases, a little ionic species may be inserted into the rod segments through ion−dipolar interactions between the ester oxygens of the rod segments and lithium cations, which gives rise to a steric effect that hinders molecular packing of the rods.

(12) Percec, V.; Lee, M. *Macromolecules* **1991**, *24*, 2780.

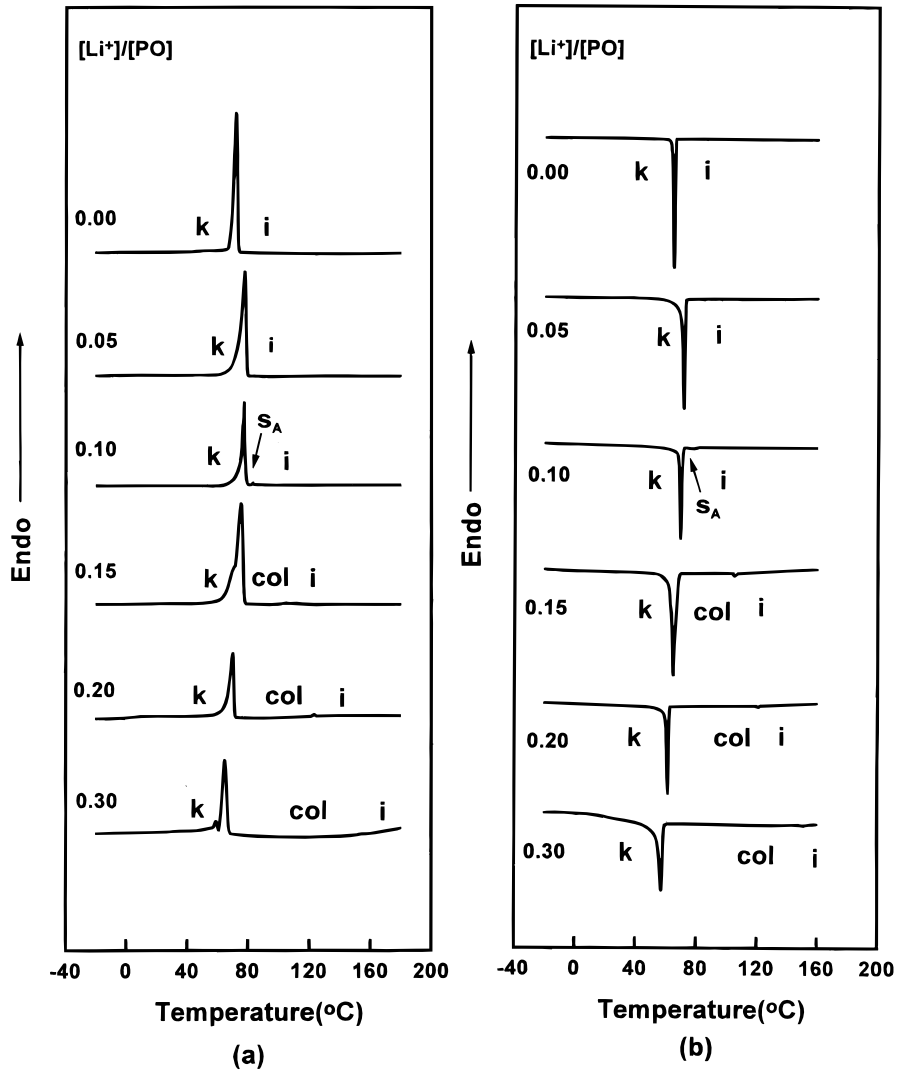

Figure 4. DSC traces (10 °C min^{-1}) recorded during the heating scan (a) and the cooling scan (b) of **12-22**.

This could result in the decrease in the enthalpy change with increasing salt concentration. Additional experiments which support these assumptions are in progress.

Induction of a smectic A mesophase in a non-liquid-crystalline coil−rod−coil triblock molecule containing poly(propylene oxide) upon complexation is interesting. This is most probably due to enhanced microphase segregation between hydrophobic segments and poly(propylene oxide) coil segments caused by transformation from a dipolar medium to an ionic medium in poly(propylene oxide) coil segments. This allows for increasing lateral intermolecular interactions of the aromatic rods. As a result, a layered smectic mesophase can be induced, as displayed by the lithium complexes of **7-22.**

Thermal behavior of the complexes of 12-22 with $LiCF_3SO_3$. Figure 4 presents the DSC traces obtained from the heating (Figure 4a) and cooling scans (Figure 4b) of coil−rod−coil molecule **12-22** and its complexes with 0.05−0.30 mol of $LiCF_3SO_3$ per propylene oxide unit of **12-22**. The phase transitions and associated enthalpy changes are summarized in Table 2. As shown in Figure 4 and Table 2, the coil−rod−coil molecule **12-22** and the complex with 0.05 mol of $LiCF_3SO_3$ exhibit only a crystalline melting transition. In contrast, the addition of 0.10 mol of $LiCF_3SO_3$ induces the formation of an enantiotropic liquid crystalline phase. The complex with 0.10 mol of $LiCF_3SO_3$ exhibits a crystalline melting transition at 77.8 °C followed by a smectic A mesophase which transforms into an isotropic liquid at 83.4 °C. On cooling from the isotropic liquid, the focal conic fan texture can be observed as shown in Figure 5a.

Table 2. Thermal Transitions of 12−22 and Its Complexes with Lithium Triflate

complex $[LiCF_3SO_3]$/[PO]	phase transitions (°C) and corresponding enthalpy changes (kJ/mol)[a]	
	heating	cooling
0.00	k 72.5 (69.1) i	i 64.7 (68.6) k
0.05	k 78.2 (37.4) i	i 71.2 (36.6) k
0.10	k 77.8 (21.9) s_A 83.4 (0.3) i	i 77.4 (0.4) s_A 69.3 (23.4) k
0.15	k 76.5 (17.3) col 107.5 (0.2) i	i 105.3 (0.2) col 64.7 (18.4) k
0.20	k 70.2 (11.6) col 123.3 (0.2) i	i 120.9 (0.2) col 61.3 (11.9) k
0.30	k 64.8 (5.4) col 153.7 (0.1) i	i 151.3 (0.2) col 57.2 (5.9) k

[a] k, crystalline; s_A, smectic A; col, columnar; i, isotropic.

In significant contrast to the phase behavior of the complex with 0.10 mol of $LiCF_3SO_3$, the complexes with 0.15−0.30 mol of $LiCF_3SO_3$ do not exhibit a smectic phase but rather an enantiotropic hexagonal columnar phase. The complex with 0.15 mol of $LiCF_3SO_3$ melts into a mesophase which is stable up to 107.5 °C. On

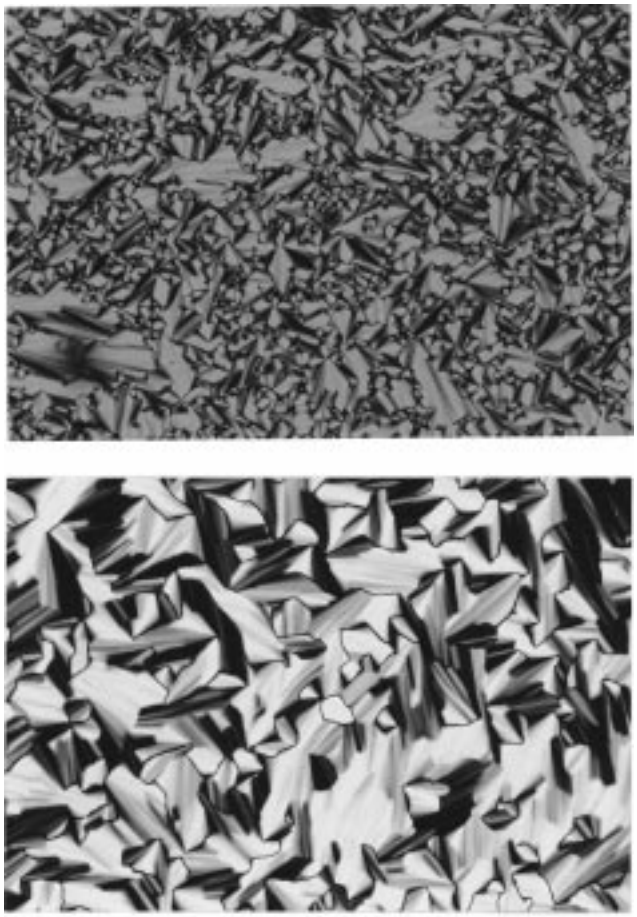

Figure 5. Representative optical polarized micrographs (65×) of the texture exhibited by (a, top) the s_A mesophase of the complex of **12-22** with 0.10 mol of $LiCF_3SO_3$ at 75 °C on the cooling scan and (b, bottom) the hexagonal columnar mesophase of the complex of **12-22** with 0.15 mol of $LiCF_3SO_3$ at 100 °C on the cooling scan.

cooling from the isotropic liquid, the formation of a pseudo-focal-conic texture can be observed as shown in Figure 5b. This is characteristic of a disordered hexagonal columnar mesophase exhibited by conventional discotic liquid crystals.[13] This observation is also in good agreement with the result observed for the hexagonal columnar mesophase exhibited by the lithium complexes of rod−coil molecules based on poly(ethylene oxide).[5] The complexes with both 0.20 and 0.30 mol of $LiCF_3SO_3$ show phase behavior similar to that of one the complex 0.15 mol of $LiCF_3SO_3$.

To confirm the assignments of the phases, small-angle X-ray scattering (SAXS) experiments were performed with the complex of **12-22** with 0.20 mol of $LiCF_3SO_3$ at various temperatures (Figure 6). In the crystalline phase at 31 °C, the complex displays the intense fundamental and its second and third harmonic reflections with q spacings of 0.56, 1.11, and 1.65 nm^{-1}, respectively. The ratio of their positions indicates that the complex exhibits a lamellar structure at its crystalline state. The X-ray diffraction pattern in the mesophase at 100 °C displays a strong and a weak reflection with q spacings of 0.61 and 1.06 nm^{-1} whose SAXS pattern

(13) Destrade, C.; Foucher, P.; Gasparoux, A.; Tihn, N. H. *Mol. Cryst. Liq. Cryst.* **1984**, *106*, 121.

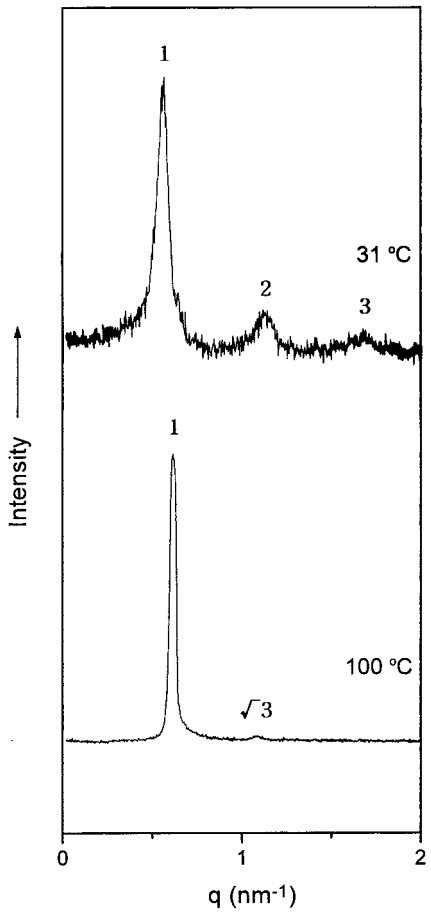

Figure 6. Small-angle X-ray diffraction patterns of the complex of **12-22** with 0.20 mol of $LiCF_3SO_3$ plotted against q ($q = 4\pi \sin\theta/\lambda$). The curves show the data obtained at 31 and 100 °C, respectively.

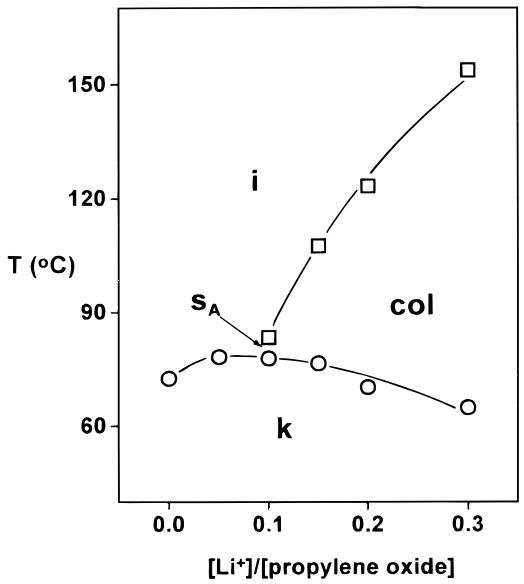

Figure 7. Dependence of the phase-transition temperatures of **12-22** and its complexes with lithium triflate on [$LiCF_3SO_3$]/[propylene oxide]. Data are from the heating scan. (○) T_m, (□) T_i.

obeys the ratio of 1:√3, which is characteristic of the two-dimensional hexagonal structure. This result together with optical microscopic observations supports that the complex of **12-22** with 0.20 mol of $LiCF_3SO_3$

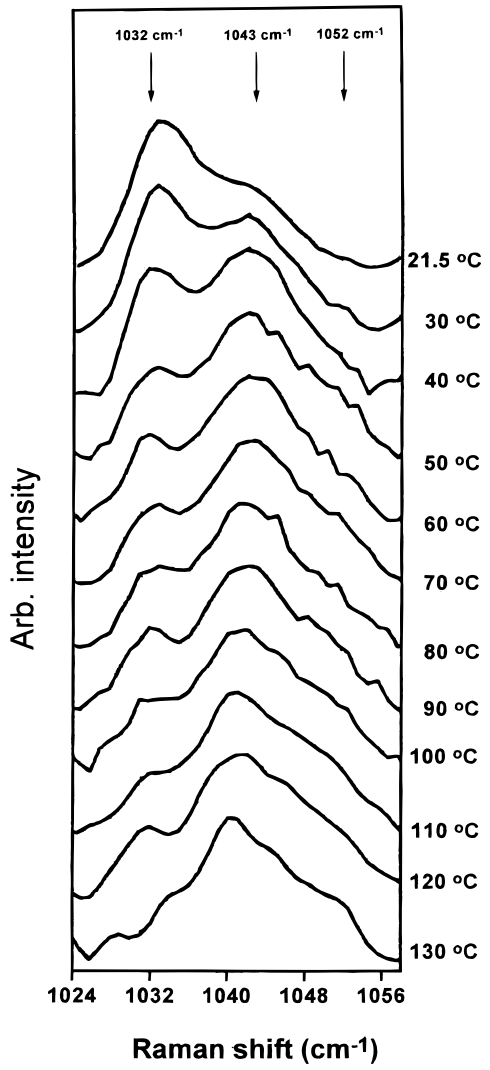

Figure 8. SO_3 symmetric stretching region for the complex of **12-22** with 0.20 mol of $LiCF_3SO_3$ at various temperatures.

displays a hexagonal columnar mesophase with a lattice constant of 11.8 nm.

Figure 7 presents the dependence of the melting and mesophase−isotropic transition temperatures obtained from the DSC heating scan as a function of salt concentration. The DSC results show that the isotropization temperatures increase drastically with the increase in the salt concentration, while the crystalline melting transition temperatures show little dependence on the salt concentration. Consequently, the range of mesophase stability increases with increasing salt concentration in the complex. This is most probably due to the increase in polarity of the poly(propylene oxide) segments generated by complexation leading to enhanced microphase segregation between each block as discussed earlier. The enhanced thermal stability of the mesophase via complexation was also confirmed for the columnar mesophase displayed by both taper-shaped[14] and rod-shaped molecules.[5]

The results described above indicate that the complexation of the non-liquid-crystalline coil−rod−coil triblock molecules with $LiCF_3SO_3$ can induce liquid crystalline phases. The primary difference between the complexes derived from **7-22** and **12-22** consists of their complexation ability to induce a mesophase. Induction of a mesophase requires 0.05 mol of $LiCF_3SO_3$ for **7-22** containing poly(propylene oxide) with a DP of 7 and at least 0.10 mol of $LiCF_3SO_3$ for **12-22** containing poly(propylene oxide) with a DP of 12. This result demonstrates that the coil−rod−coil molecule based on a longer poly(propylene oxide) coil induces the formation of a mesophase at higher salt concentrations. This can be attributed to higher conformational disorder of the melted poly(propylene oxide) chain in **12-22,** and thus **12-22** needs a greater amount of $LiCF_3SO_3$ to maintain molecular order in the melt state. Interestingly, the complexation of **12-22** with more than 0.15 mol of $LiCF_3SO_3$ induces the formation of a hexagonal columnar mesophase, in contrast to that of **7-22**. This result suggests that induction of a columnar phase through complexation requires a higher volume fraction of coil segments in a rod−coil system, which is qualitatively consistent with the results predicted by theory.[2]

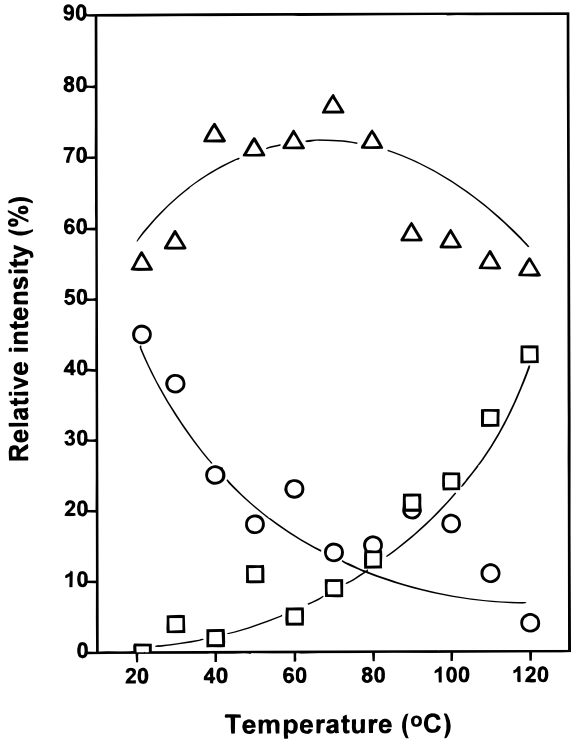

Figure 9. Temperature dependence of the relative intensity. (○) Free $CF_3SO_3^{-1}$ anion; (△) ion pair; (□) ionic aggregate.

Raman Spectroscopic Study. To investigate the role of added lithium triflate for induction of a columnar phase in the coil−rod−coil molecule, we have performed Raman spectroscopic measurements with the complex of **12-22** with 0.20 mol of $LiCF_3SO_3$ at different temperatures. Raman spectroscopy has already been successfully used to investigate fundamental questions of ionic association in polymer−salt complexes.[15] Raman scattering spectra corresponding to the SO_3 stretching mode, which is sensitive to the ionic interactions, are shown in Figure 8. The Raman bands in this spectral

(14) Percec, V.; Johansson, G.; Heck, J.; Ungar, G.; Batty, S. V. *J. Chem. Soc., Perkin Trans. 1* **1993**, 1441. (b) Percec, V.; Thomzos, D.; Heck, J.; Blackwell, H.; Ungar, G. *J. Chem. Soc., Perkin Trans. 2* **1994**, 31.

(15) Papke, B. L.; Ratner, M. A.; Shriver, D. A. *J. Electrochem. Soc.* **1982**, *129*, 1694.

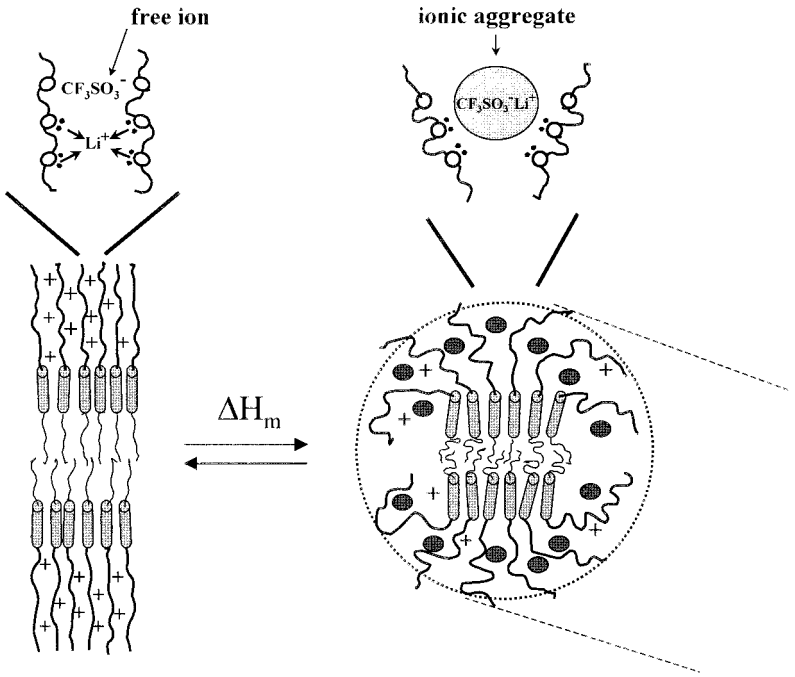

Figure 10. Schematic illustration of the formation of a cylinder responsible for the generation of the columnar mesophase from the crystalline lamellar phase of the complex of **12-22** with 0.20 mol of $LiCF_3SO_3$. Pluses represent lithium ions coordinated with oxygens; gray ovals, ionic aggregates.

region are responsible for triflate anions in various states of ionic association resulting from ether oxygen−salt interactions. The assignments of the 1033 cm^{-1} band to free ions, the 1043 cm^{-1} band to ion pairs, and the 1053 cm^{-1} band to ionic aggregates follow from the results described previously.[16] Here, free ion refers to the triflate species with no degree of ionic association. The intensity associated with each species was resolved by curve fitting, and the ratio of the intensity contribution of each species to the total intensity was calculated. These data are plotted as a function of temperature and are presented in Figure 9.

As can be seen in Figure 9, several trends can be observed. The intensity of the ionic aggregate band at 1053 cm^{-1} increases, while the intensity of the free ion band at 1033 cm^{-1} decreases drastically with increasing temperature. No significant trend is observed in the intensity contributed from the ion pairs as compared with changes found for the free ion band and the ionic aggregate band. These results suggest that the number of ionic aggregates dissolved in the microphase-segregated poly(propylene oxide) segments increases with increasing temperature, while ion−dipolar interactions between ether oxygens and ions decrease. This behavior is consistent with the results observed conventional poly(ethylene oxide)−lithium triflate complexes.[16−18]

On the basis of the experimental results obtained from the Raman spectra and the X-ray diffraction patterns, the most probable mechanism responsible for the generation of the columnar mesophase can be presented as shown in Figure 10. In the crystalline phase, the addition of $LiCF_3SO_3$ seems not to influence the volume change of the coil segments, most probably due to high ion−dipolar interactions between the poly(propylene oxide) coils and the lithium ions. This is supported by the high intensity of the free ion band observed in the Raman spectra measured at lower temperatures corresponding to a crystalline phase (Figures 8 and 9). Similar behavior was also confirmed by density measurements for the lithium complexes of rod−coil molecules based on poly(ethylene oxide).[5b]

As the temperature increases, the number of ionic aggregates increases at the expense of the free ions as reflected in the Raman spectra (Figures 8 and 9). The increased ionic aggregates would result in a large space crowding of the microphase-segregated poly(propylene oxide) segments, and thus the flexible coils grafted onto flat interfaces spread out into a larger region of space to reduce space crowding. Consequently, crystalline lamellar breaks into cylindrical micelles which allow more space for poly(propylene oxide) coils, leading to less coil stretching (Figure 10).[2] The resulting cylindrical micelles self-assemble into a hexagonal columnar mesophase as exhibited by the lithium complexes of **12-22**.

Conclusions

The results described in this paper demonstrate that the complexation of non-liquid-crystalline coil−rod−coil molecules with $LiCF_3SO_3$ can give rise to a liquid crystalline phase. The complexation of non-liquid-crystalline coil−rod−coil triblock molecule **7-22** containing poly(propylene oxide) with a DP of 7 induces a smectic A mesophase. In marked contrast, upon complexation of non-liquid-crystalline coil−rod−coil triblock molecule **12-22** containing a longer poly(propylene oxide) coil, notable phase change can be observed. The complexes display successively a crystalline phase and layered smectic A and hexagonal columnar mesophases as the highest temperature phase with increasing salt concen-

(16) (a) Petersen, G.; Jacobsson, P.; Torell, L. M. *Electrochim. Acta* **1992**, *37*, 1495. (b) Huang, W.; Frech, R. *Polymer* **1994**, *35*, 235.
(17) Yu, S.-C.; Paek, J.; Yu, K. H.; Ko, S. B.; Cho, I.-H.; Lee, M. *Bull. Kor. Chem. Soc.* **1997**, *18*, 773.
(18) Chintapalli, B.; Frech, R. *Macromolecules* **1996**, *29*, 3499.

tration. These results suggest that the control of self-assembled liquid crystalline structure as well as the induction of the liquid crystallinity is possible in the molecular rod system containing a poly(propylene oxide) coil through lithium complexation. It is especially remarkable that the rodlike molecule can organize into a columnar mesophase. This behavior can be attributed to the variation of ionic association state induced by ion−dipolar interactions.

Acknowledgment. Financial support of this work by the Ministry of Education, Republic of Korea (BSRI-97-3422), and the Korea Science and Engineering Foundation (971-0301-004-2) is gratefully acknowledged. We are also grateful to Prof. S.-C. Yu for Raman spectroscopic measurements and Prof. W.-C. Zin for X-ray measurements.

CM980070T